18
Polymer Particles

Christophe Serra

18.1
Introduction

The synthesis of polymer particles has long been the focus of a very intensive research because from painting formulations to drug delivery they cover a wide range of applications. So far, polymer particles in the range from a few microns to hundreds of microns were mainly prepared by either heterogeneous polymerization processes (suspension, supercritical fluid) or by precipitation processes in a non-solvent. However, for this specific range of sizes, these two processes induce a large particle size distribution.

On the other hand, new developments in microfabrication techniques have allowed the fabrication of very efficient emulsification microsystems. Thus, droplets or bubbles, with an extremely narrow size distribution (the coefficient of variation of the particle size distribution is typical lower than 5%), can be continuously produced and dispersed in a continuous fluid flowing within the microsystem. If the phase to be dispersed is composed of a polymerizable liquid, the droplets can be hardened downstream by either thermally or photoinduced polymerization. Depending on how complete the polymerization is within the droplet, the size of the final polymer particle is usually smaller than that of the originate droplet by 2–10% due to the higher density of the polymer. Over conventional processes, microsystem-assisted processes offer the possibility of precisely controlling not only the size of the particle but also its shape, morphology and composition.

In this chapter, we review the latest results reported in the literature concerning the microsystem-assisted synthesis of polymer particles. We first describe the most common microfabricated systems used to produce polymer particles. We then focus on the various particles (beads, capsules and other shapes and morphologies) which can be produced with each of the described microsystems.

Micro Process Engineering, Vol. 2: Devices, Reactions and Applications.
Edited by V. Hessel, A. Renken, J.C. Schouten, and J.-I. Yoshida

ISBN: 978-3-527-31550-5

18.2
Most Common Microsystems

One can distinguish between two different techniques for the production of polymer particles with microsystems: (a) emulsification of liquid monomers followed by polymerization of the subsequent monomer droplets and (b) direct polymerization through continuous flow projection photolithography.

18.2.1
Emulsification Technique

Three different types of microsystem have been reported for the emulsification of a polymerizable liquid (Figure 18.1), namely the terrace-like microchannel device, the T-junction microchannel device and the flow focusing device (FFD). The emulsification mechanism, which is similar for these three devices, proceeds from the break-up of a liquid thread into droplets when the phase to be dispersed is sheared by the continuous and immiscible phase.

The terrace-like microchannel device (Figure 18.1a) consists of a main channel in which the continuous phase flows. Several microchannels deliver the dispersed phase at the top and from both sides of the main channel. Then terraces located just below the microchannels allow the break-up of the dispersed phase thread. In T-junction microchannel devices (Figure 18.1b), the phase to be dispersed is delivered through a microchannel perpendicular to a main channel in which the continuous phase flows. Depending on the flow rates of the continuous and dispersed phases, the break-up is observed at the junction of the two microchannels

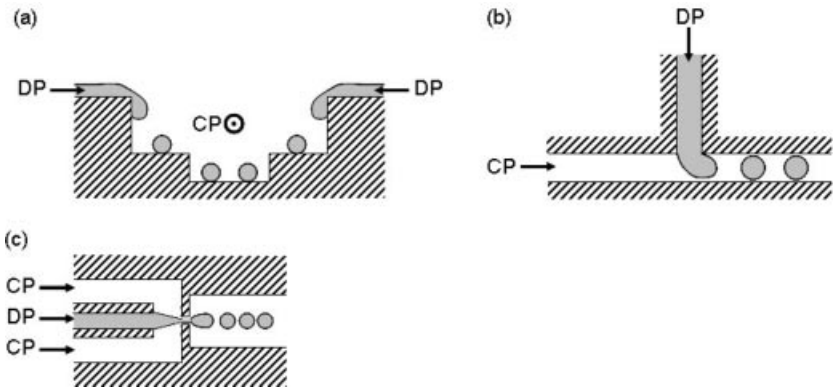

Figure 18.1 Different microsystems for the emulsification of a liquid monomer: (a) terrace-like microchannel device; (b) T-junction microchannel device; (c) flow focusing device. CP and DP are the continuous phase and the phase to be dispersed, respectively.

or further downstream. FFDs (Figure 18.1c) are based on the principle of hydrodynamic focusing. The dispersed phase flows in a central microchannel whereas the continuous phase is delivered through two side channels. In front of the central channel, a small orifice or a restriction allows the continuous phase to pinch the dispersed liquid thread, which breaks past the orifice into droplets.

Although each microsystem has its own characteristics, some general trends can be identified for the control of the particle size. Two dimensionless numbers were identified which contribute significantly to the final particle diameter: the Reynolds number (*Re*) and the capillary number (*Ca*):

$$Re = \frac{\rho V D}{\mu} \tag{18.1}$$

$$Ca = \frac{\mu V}{\gamma} \tag{18.2}$$

where ρ and μ are the fluid density and viscosity respectively, V the mean fluid velocity, D a characteristic dimension of the flow (usually the channel width) and γ the interfacial tension between the two immiscible fluids. Thus the particle diameter is primarily a function of the velocities or flow rates of the two phases. Generally, an increase in the continuous phase flow rate or a decrease in the dispersed phase flow rate induces a decrease in the mean polymer particle diameter. This diameter is also affected by the interfacial tension, with lower interfacial tension leading to smaller particles. Fluid viscosity also plays an important role. An increase in the continuous phase viscosity or a decrease in that of the dispersed phase is usually followed by a decrease in the final particle size. Finally, it was observed that a reduction in the characteristic dimension of the microsystem, e.g. the channel width for the terrace-like microchannel and T-junction devices and the orifice width for the MFFD, generates smaller particles.

18.2.2
Projection Photolithography Technique

This unique technique consists in the UV irradiation, through the objective of an optical microscope, of a monomer solution flowing within a microchannel. A mask placed in the field-stop plane of the microscope allows polymerization and "printing" of the desired particle shape to the flowing monomer solution. This technique relies on two necessary conditions: (1) polymerization should be fast enough that particles do not move significantly during their irradiation, otherwise shape deformation occurs, and (2) the presence of a thin layer of oxygen near the microchannel walls, which inhibits locally the polymerization and allows the particle to flow with the monomer solution. The microchannel is made of polydimethylsiloxane (PDMS), the permeability of which to oxygen allows the establishment of the oxygen inhibition layer.

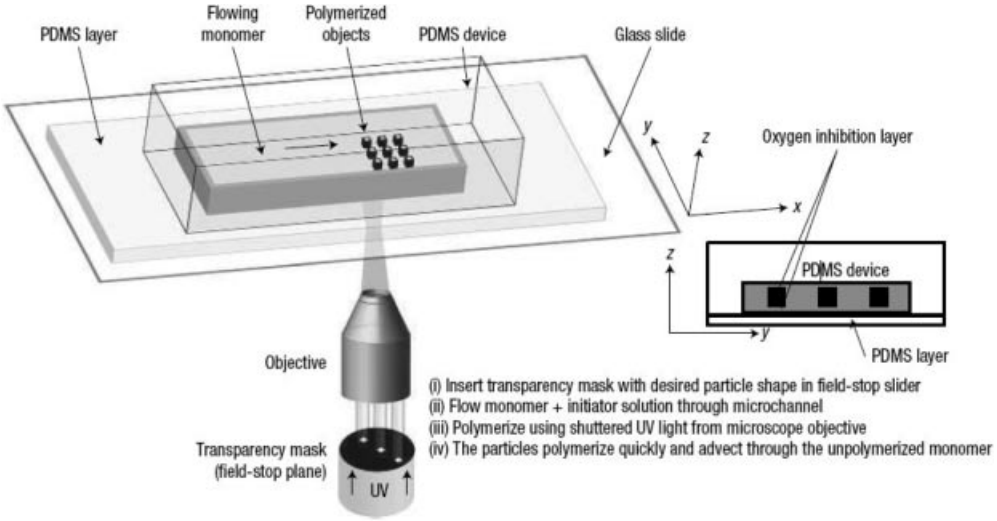

Figure 18.2 Schematic representation of continuous flow projection photolithography. From Ref. [21].

18.3 Examples of Various Polymer Particles Produced with Microsystems

18.3.1 Terrace-like Microchannel Devices

Nakajima and coworkers [1, 2] were the first to propose a microfabricated system for the preparation of polymer particles. Their terrace-like microchannel device (Figure 18.3, top), originally developed for the emulsification of different oil-in-water or water-in-oil cells [3], was used for the production of polydivinylbenzene spherical particles. An aqueous solution containing 0.2 wt.% of a surfactant (sodium dodecyl sulfate, SDS) was flowing in the main channel (3.8 mm long × 14 mm wide). The side microchannels (12 μm width, 2 μm depth) delivered the dispersed phase composed of a solution of divinylbenzene (DVB) and 2 wt.% of a thermal initiator (benzoyl peroxide, BPO). The terraces had a width of 32 μm and a length of 25 μm. The resulting emulsion was then recovered and mixed with an aqueous solution containing 4 wt.% of poly(vinyl alcohol) (PVA). This solution was finally heated to 90 °C in order to convert the DVB droplets into solid polymer beads (Figure 18.3, bottom). By modifying the geometric parameters of the microchannels and terraces, the authors obtained beads of poly(DVB) with diameters ranging from 4 to 100 μm and having coefficients of variation lower than 9%.

In another study, Nakajima and coworkers [4] used this microsystem for the production of polymer gel particles from *N*-isopropylacrylamide (NIPam). The

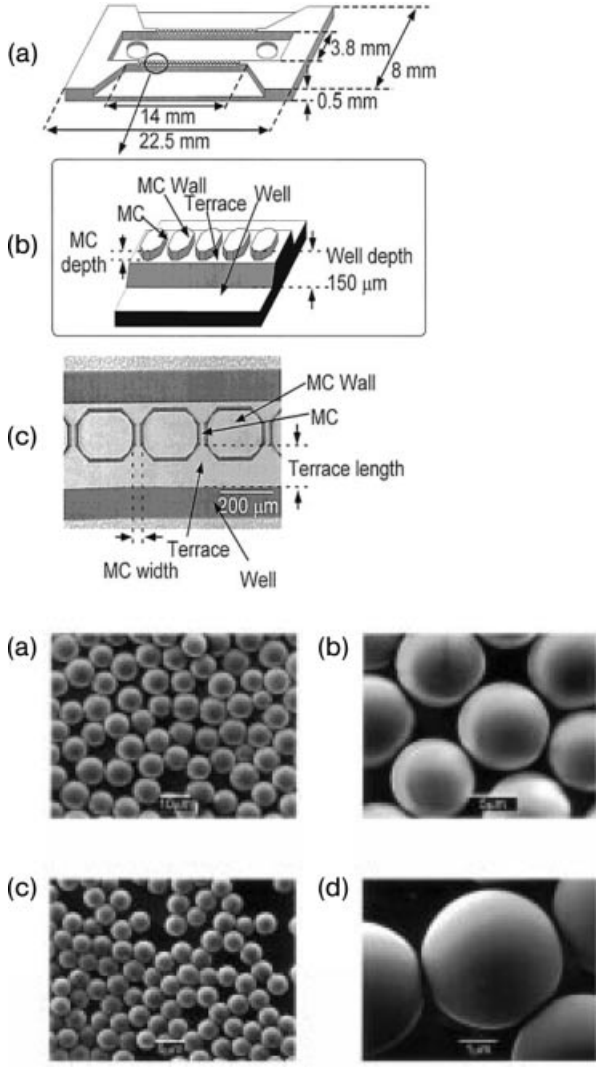

Figure 18.3 Top: schematic drawing of the terrace-like microchannel device. From Ref. [2]. Bottom: SEM images of poly (DVB) beads at different magnifications. From Ref. [1].

continuous phase was an isooctane solution containing 5 wt.% of a surfactant (Span 80). The dispersed phase was formulated with a photoinitiator (ammonium persulfate, APS) so that UV-induced gelation transformed monomer droplets into gel microspheres. These gel particles had an average size ranging from 3 to 100 μm and a relative standard deviation lower than 5%.

18.3.2 T-junction Microchannel Devices

The first application of a T-junction microchannel device [5, 6] for the production of functional polymer beads was reported by Nisisako *et al.* [7]. The channels were machined into a quartz plate which was covered with another quartz plate by fusion bounding. This T-junction microchannel device (Figure 18.4, top) was then used for the emulsification of a solution of 1,6-hexanediol diacrylate and 1 wt.% of a photoinitiator (Darocur 1173, Ciba) with an aqueous solution containing 2 wt.% of PVA. The emulsion was subsequently recovered outside the microsystem in a beaker. Then the monomer droplets were polymerized under UV irradiation. By increasing the flow rate of the continuous phase (Q_c) from 1 to 27 mL h^{-1}, for a constant dispersed phase flow rate of $Q_d = 0.1$ mL h^{-1}, the authors decreased the average size of the polymer beads from 125 to 30 μm (Figure 18.4, bottom). The particle size distribution was fairly narrow (CV <2%); however, satellite droplets of smaller diameter were also generated in the wake of the primary droplets. A specific study on the influence of the flow rate of the dispersed phase, at fixed values of the continuous phase flow rate, showed a flow diagram in which three regions were identified. At low values of Q_c, the continuous and dispersed liquids flow in parallel streams; for intermediate values of Q_c, monodisperse droplets of monomer are formed; finally, at high values of Q_c, disordered patterns are observed and polydisperse droplets are formed.

Following the work of Nisisako *et al.*, non-spherical polymer particles were synthesized by Doyle and coworkers [8]. However, several features distinguish this approach from the previous T-junction microchannel device. Non-spherical particles were obtained after *in situ* UV-induced photopolymerization of plug droplets. These droplets were obtained for a specific combination of continuous and dispersed flow rates and by employing a main microchannel the dimensions of which do not allow spherical relaxation (Figure 18.5, top). Thus, a UV-sensitive liquid photopolymer (NOA60, Norland Products) was emulsified with water containing 1 wt.% of a surfactant (SDS) into plug droplets at the T-junction. The device was obtained by PDMS replication of a positive relief of the microchannel patterned in SU-8 photoresist deposited on a silicon wafer and sealed with a glass slide by plasma bonding. Plug-shaped particles were then obtained after UV irradiation (Figure 18.5, top). To obtain disk-like particles (Figure 18.5, bottom), the plug droplets must adopt a discoid shape before being exposed to the UV radiation. This is achieved by widening the main microchannel from 40 to 200 μm and by reducing the channel height from 38 to 16 μm (Figure 18.5, bottom). As for polymer beads, the sizes of these non-spherical polymer particles can be tuned by adjusting the flow rates of the continuous and dispersed phases.

The T-junction microchannel device was also used for the preparation of molecularly imprinted polymers (MIP) [9]. The T-junction (200 μm wide × 200 μm deep) was drilled in a polycarbonate sheet (Figure 18.6, top). The main channel opens into a wider and spiral-like channel (500 μm wide × 300 μm deep). The device was sealed with a 100 μm thick acetate foil which was bonded with UV-curable epoxy resin.

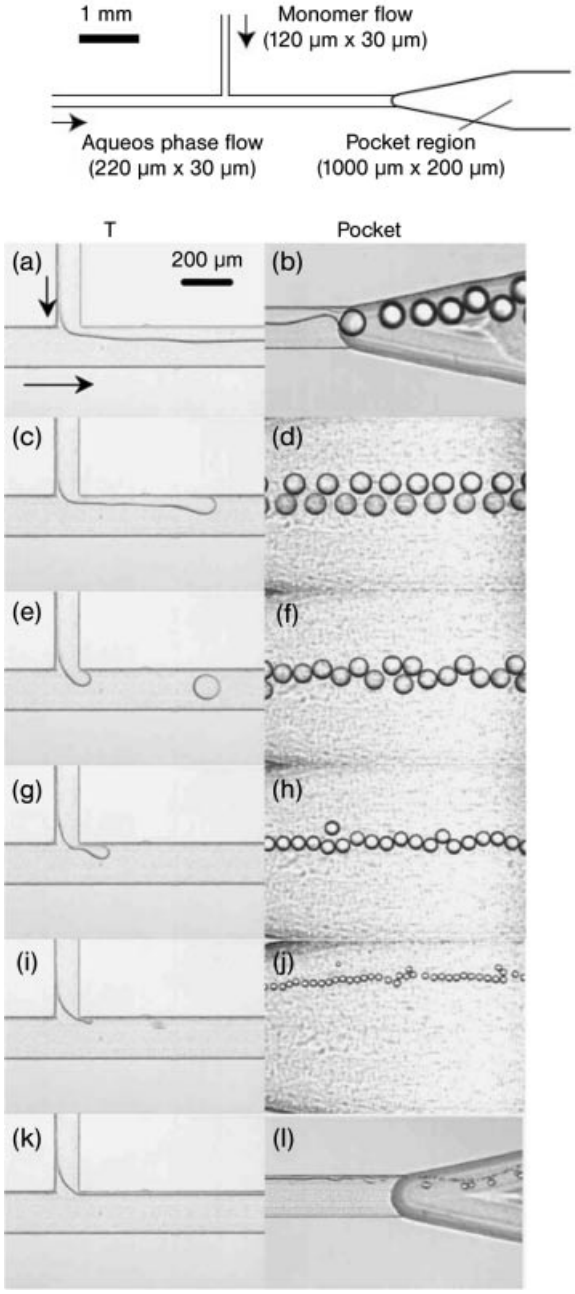

Figure 18.4 Top: design and dimensions of the T-junction microchannel device used for the synthesis of poly(1,6-hexanediol diacrylate) beads. Bottom: images of droplet formation for different continuous phase flow rates at a fixed flow rate of the dispersed phase ($Q_d = 0.1\,mL\,h^{-1}$): $Q_c =$ (a, b) 0.5, (c, d) 1.0, (e, f) 2.0, (g, h) 4.0, (i, j) 18.0, (k, l) 22.0 $mL\,h^{-1}$ From Ref. [7].

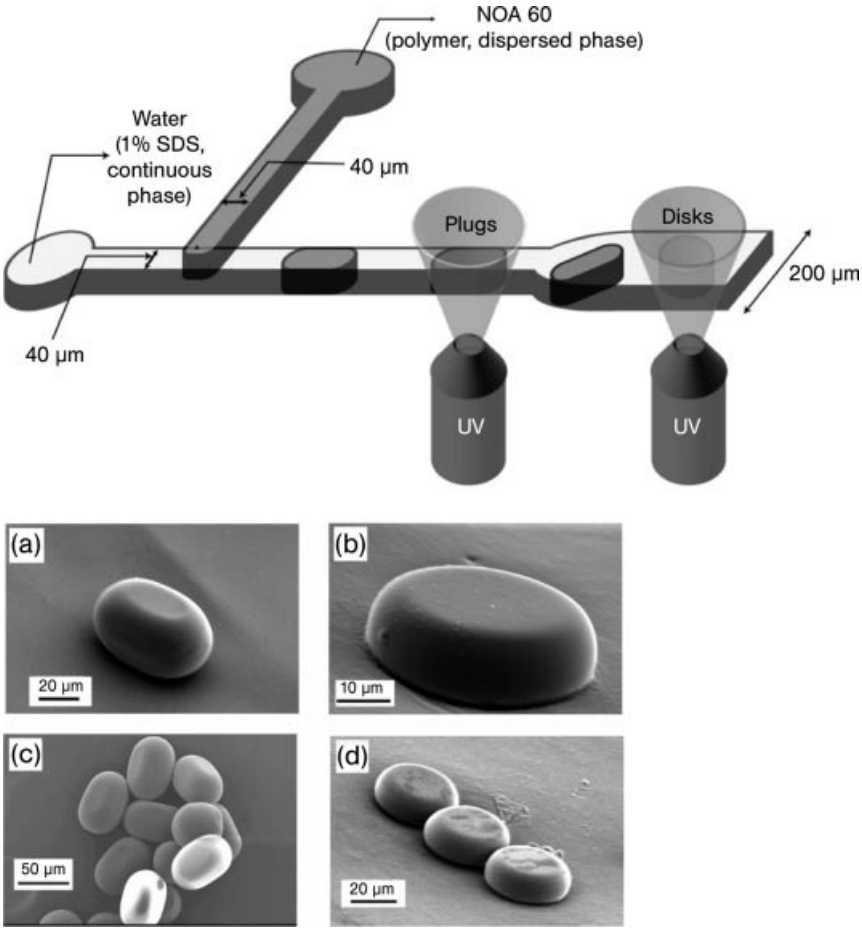

Figure 18.5 Top: schematic depicting the T-junction microchannel device for production of non-spherical polymer particles. Bottom: SEM images of plug-shaped particles (a, c) and disk-like particles (b, d). From Ref. [8].

The dispersed phase was injected through a 35 µm hole drilled in the acetate sheet. The formulation for the MIP synthesis, containing the template [(*R*,*S*)-propranolol], the monomer (methacrylic acid, MAA), the crosslinker (trimethylolpropane trimethacrylate, TRIM), the photoinitiator (2,2-dimethoxy-2-phenylacetophenone, DMPAP) and a porogenic solvent (acetonitrile), was emulsified at the T-junction with a mineral oil (heavy white) and then photopolymerized by UV irradiation in the spiral-like channel. The resulting MIP particles were compared with those obtained with a conventional batch process. The continuous microsystem-assisted process led to near-monodisperse particles (CV <2%), whereas the conventional process gave particles having a broad range of sizes (CV >10%). The same conclusion holds for

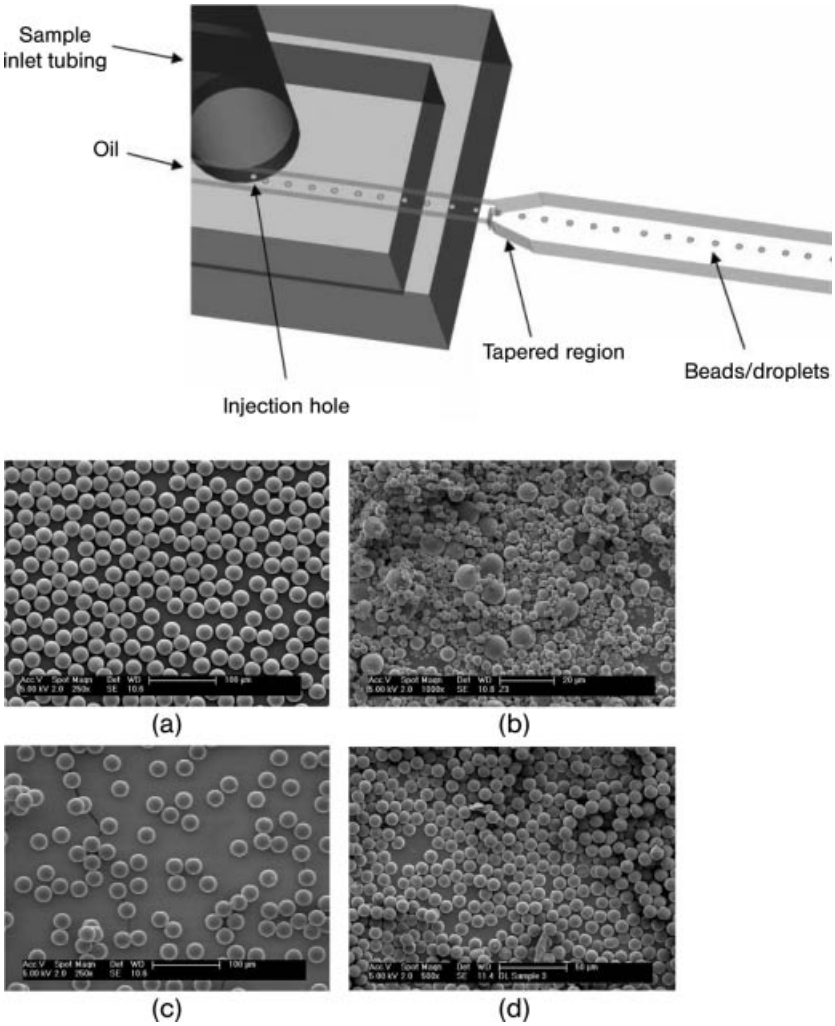

Figure 18.6 Top: schematic drawing of the T-junction microchannel device for production of MIP particles. Bottom: SEM images of MIP particles obtained with the mineral oil (a, b) and perfluorocarbon (c, d) as the continuous phase in the T-junction microchannel device (a, c) and in a conventional batch reactor (b, d). From Ref. [9].

another formulation based on the emulsification in a perfluoro(1,3-dimethylcyclohexane) continuous phase (Figure 18.6, bottom). The authors also stressed that the microsystem-assisted process allow the synthesis of MIP particles with larger sizes, in contrast to the conventional process. Takeuchi and coworkers [10] also reported the successful synthesis of atrazine-MIP spherical and monodisperse particles but with a Y-junction microchannel device.

18.3.3
Flow Focusing Devices

The very first flow focusing device was developed by Stone and coworkers [11] and was used for the emulsification of water in silicone oil. The geometry of this device is depicted in Figure 18.7 and was obtained after replication of a positive relief of the microchannels patterned in SU-8 photoresist. The authors named this FFD a "microfluidic flow focusing device" (MFFD). A few years after the development of this microsystem, Kumacheva and coworkers [12] used an MFFD (Figure 18.7, top left) made out of PDMS or polyurethane (PU) for the emulsification and polymerization of several multifunctional acrylates: ethylene glycol dimethacrylate (EGDMA),

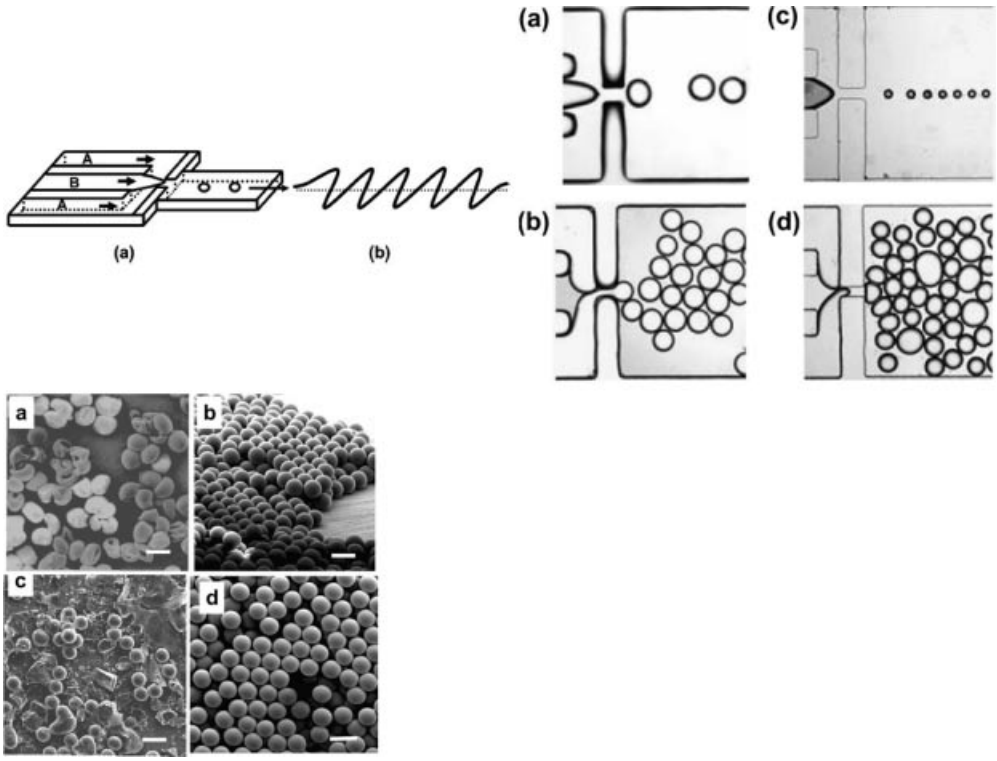

Figure 18.7 Top Left: schematic drawing of the MFFD. Top right: optical images of MAOP-DMS emulsification with methylene blue dye labeled water in an MFFD made of PU (a, b) or PDMS (c, d); MAOP-DMS was delivered to the central channel (a, d) or the side channels (b, c). Bottom: SEM images of poly(TPGDA) particles (a, b, c) and poly(PETA-3) particles (d) obtained with 2 (a),4 (b, d) and 6 wt.% (c) of initiator (HCPK). From Ref. [12].

tri(propylene glycol) diacrylate (TPGDA), pentaerythritol triacrylate (PETA-3) and pentaerythritol tetraacrylate (PETA-4) and one monofunctional monomer: methacryloxypropyldimethylsiloxane(MAOP-DMS). Once emulsified, the dispersed phase was UV polymerized downstream in a wavy channel thanks to the presence of a photoinitiator (1-hydroxycyclohexyl phenyl ketone, HCPK) in the droplet phase. Multifunctional monomers were used on the one hand to obtain solid particles and on the other to reduce the time of photopolymerization as much as possible to make it appropriate with respect to the residence time in the wavy channel (30 s to 15 min). Depending on the propriety of the device's material and the fluids, "phase inversion" can be observed, i.e. when the phase to be dispersed becomes a continuous phase. MAOP-DMS presents a higher affinity for hydrophobic materials. Hence its emulsification in an MFFD made of PDMS led to the formation of water droplets (Figure 18.7, top right, d), whereas droplets of MAOP-DMS were produced in an MFFD made of a hydrophilic material such as PU (Figure 18.3, top right, a). Hence, provided that the material of the MFFD is correctly chosen, one obtains polymer beads at the exit of the device. However, the particle hardness and monomer conversion depend strongly on the amount of initiator. For low concentrations (<2 wt.%), the monomer was not fully polymerized. The result is the formation of a rigid skin which collapses under vacuum (Figure 18.7, bottom, a). For high concentrations (>6 wt.%), the large amount of heat released by the polymerization made the particles explode (Figure 18.7, right, c). In between, there is a range of initiator concentrations for which particles with a smooth surface are obtained (Figure 18.7, bottom, b, d).

The authors also synthesized non-spherical poly(TPGDA) particles (Figure 18.8, middle). This was achieved by reducing the dimensions of the outlet microchannel so that monomer droplets adopt a disk-like or plug shape before being UV irradiated (Figure 18.8, left).

Following up the production of disk-like monomer droplets, Kumacheva *et al.* [13] organized the droplets into 2D lattices in the outlet channel as shown in Figure 18.8 (right). Depending on the size of the channel and droplets, lattices with different numbers of columns were obtained. Finally, the lattices were trapped in the solid state by UV irradiation and formed a highly periodic array of disk-like polymer particles.

This MFFD proved to be extremely versatile for the production of multicomponent polymer-based beads (Figure 18.9). By simply admixing the monomer phase with the appropriate reagent, Kumacheva and coworkers [14, 15] were able to incorporate dye, quantum dots and liquid crystals into poly(TPGDA) particles and to synthesize porous microspheres and also copolymer particles made of TGPA and acrylic acid (AA).

By adding two side channels to the original MFFD (Figure 18.10, left), Kumacheva and coworkers [16] achieved the flow focusing of three immiscible fluids. The result was the generation of multiple emulsions, i.e. droplets-in-droplet structure (Figure 18.10, right). The fluid A (silicone oil, SO) flowing in the central channel was emulsified in multiple droplets engulfed in a droplet of a polymerizable fluid B

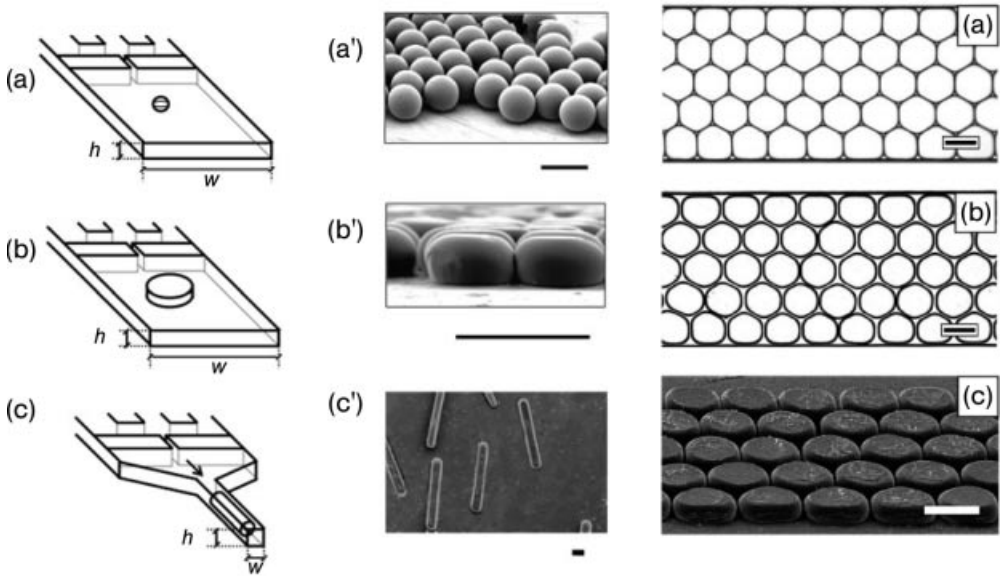

Figure 18.8 Left: schematic drawing of the MFFD used to obtain polymer particles with different shapes. Middle: optical images of poly(TPGDA) particles having a spherical (a′), discoid (b′) and ellipsoidal (c′) shape. Right: optical microscopy images of dimethacrylate oxypropyldimethylsiloxane droplets before (a) and after (b) photopolymerization; SEM image (c) of the disk-like polymer particle array. From Ref. [13].

(TGPDA) surrounded by the continuous phase fluid A (aqueous SDS solution). The downstream photopolymerization of the monomer droplets led to core–shell particles having various morphologies (Figure 18.11, top). By tuning the three fluid flow rate ratios, the authors achieved control over the core–shell particle size, shell thickness and the diameter and number of cores per particle. The different morphologies adopted by the core–shell particles was revealed in a ternary phase-like diagram where each axis represents the flow rate of the three liquids normalized to the total flow rate (Figure 18.11, bottom).

Two modified versions of the MFFD allowed Kumacheva and coworkers [17] to achieve the production of Janus and ternary particles. The morphology of these particles is such that two (Janus) or three (ternary) different materials compose the particle. These particles are obtained after *in situ* photoinitiated polymerization of multiphase droplets. To obtain these droplets, one has to establish first a co-flow between three (Janus) or four (ternary) fluids, as shown in Figure 18.12 (top). Thus, the Janus droplet generator is composed of two central channels in which flow two different monomer solutions formulated with a photoinitiator and two side channels delivering the continuous 2 wt.% SDS aqueous solution. The ternary droplet generator differs from the latter by the three central channels allowing the delivery of at least two different monomer solutions. By emulsifying a solution M1 of MAOP-DMS and

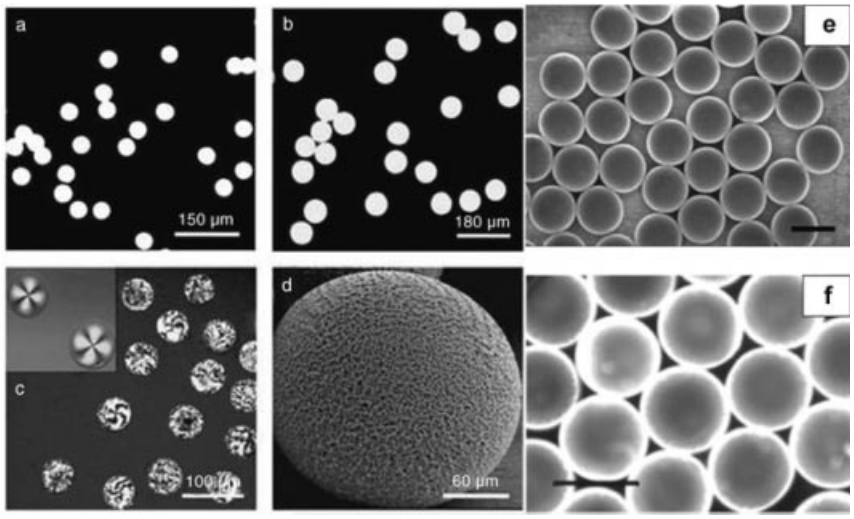

Figure 18.9 Examples of multicomponent polymer-based beads synthesized in an MFFD: poly(TPGDA) microspheres labeled with 4-amino-7-nitrobenzo-2-oxa-1,3-diazole dye (a) or CdSe quantum dots (b), poly(TPGDA) microspheres incorporating 4-cyano-4′-pentylbiphenyl liquid crystal as seen by polarization microscopy (c), SEM image of a porous poly(TPGDA) microsphere (d), SEM image of a poly(TPGDA–AA) copolymer particles (e), fluorescent microscopy image of copolymer particles following their bioconjugation with FITC-BSA (f). From Refs [14, 15].

a solution M2 composed of pentaerythritol triacrylate (45 wt.%), poly(ethylene glycol) diacrylate (45 wt.%), acrylic acid (5 wt.%) and a small amount of florescent monomer NBD-methacrylate (NBD-MA), both formulated with 4 wt.% of HCPK, Janus and ternary particles were obtained after typically 2–50 s of UV irradiation. Images of the particles are shown in Figure 18.12 (bottom).

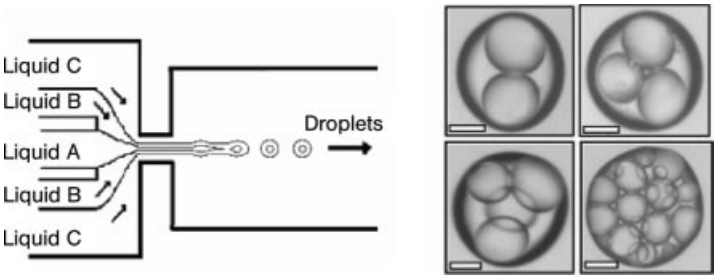

Figure 18.10 Left: schematic drawing of an MFFD for production of multiple emulsions. Right: optical microscopy images of TPGDA droplets containing several SO cores. From Ref. [16].

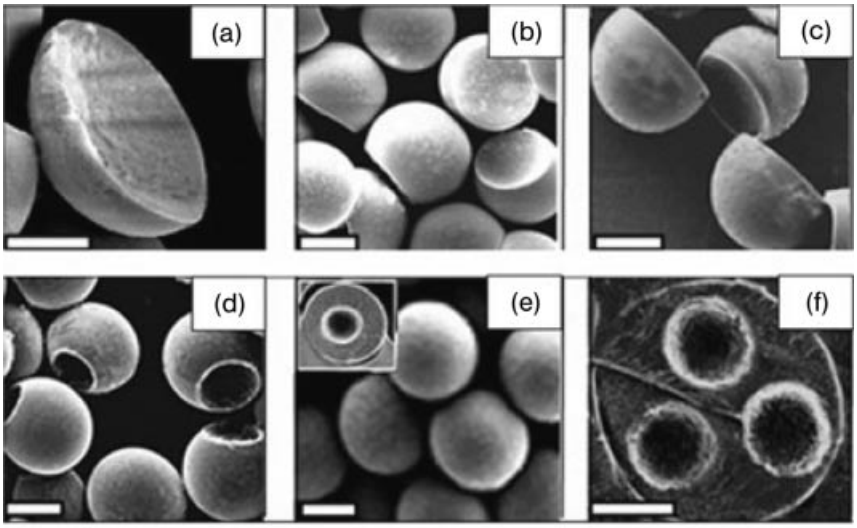

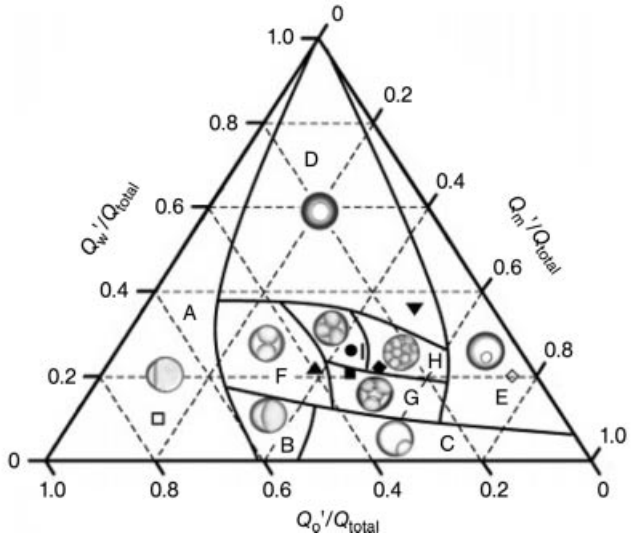

Figure 18.11 Top: SEM images of different poly (TPGDA) core–shell particles after removing SO cores (a, b, c, d); cross-section of a core–shell particle containing one (e, inset) or three (f) SO cores. Bottom: ternary phase-like diagram of hydrodynamic conditions used in the production of droplets with various morphologies. Q_w, Q'_m, Q'_o and Q_{tot} are the water, monomer, oil and total flow rates, respectively. Letters in the diagram correspond to core–shell structures revealed in the images on top. From Ref. [16].

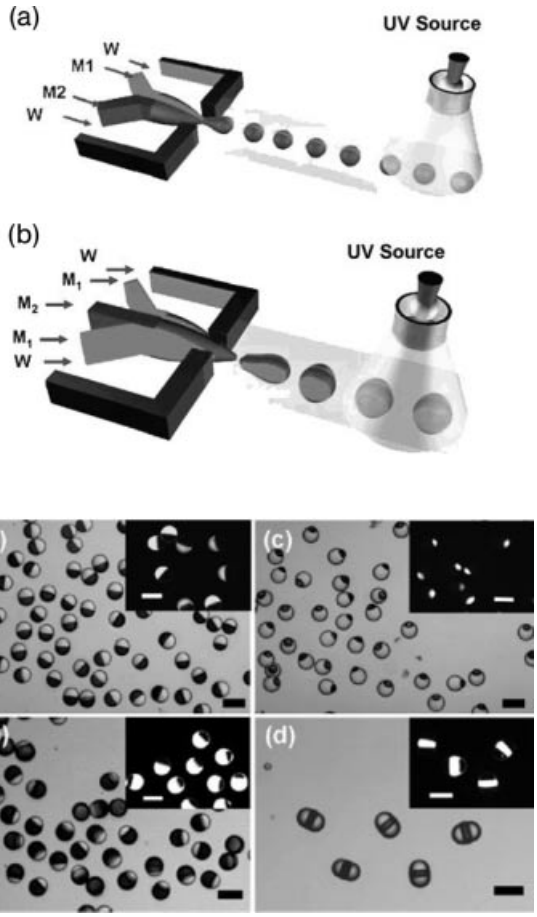

Figure 18.12 Top: schematic drawing of modified MFFDs for production of Janus (a) and ternary (b) droplets. Bottom: optical microscopy images of Janus (a, b, c) and ternary (d) particles. Bright and dark phases are polymers of M1 and M2, respectively. Insets show fluorescence microscopy images of the corresponding particles. From Ref. [17].

In addition to the MFFD, another flow focusing device was first reported by Nisisako *et al.* [7] for the production of polymer particles. In that device, the hydrodynamic focusing of the dispersed phase is achieved thanks to two sheath fluids coming from both sides of the microchannel in which flows the dispersed phase (Figure 18.13, top). This sheath-flow microfluidic device (SFMD), etched in a quartz glass slab, was used in conjunction with a Y-junction to emulsify Janus droplets (Figure 18.13, middle). Two differently colored solutions of isobornyl acrylate (IBA) admixed with a small amount of a thermal initiator were fed to the

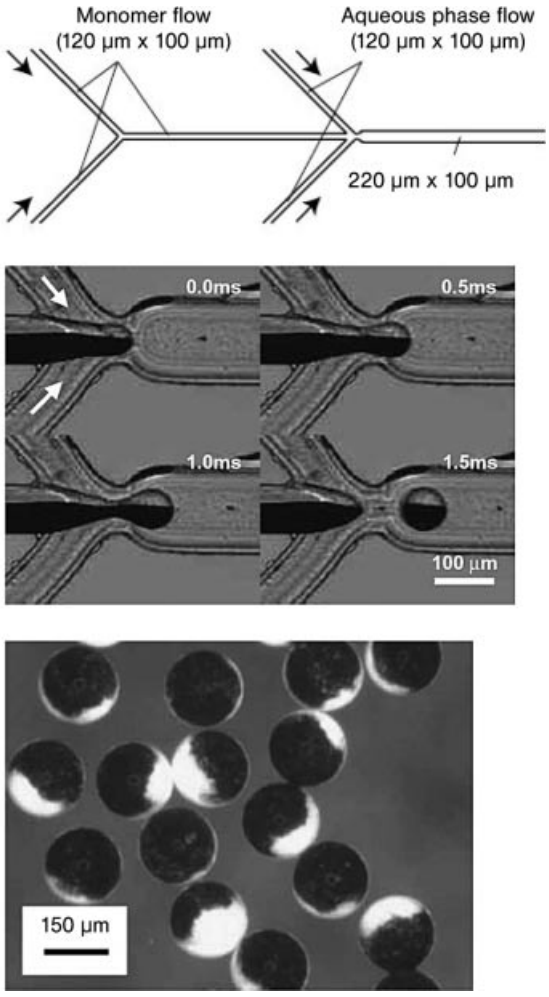

Figure 18.13 Design and dimensions of the Y-junction and sheath junction used for the production of Janus droplets (top). Optical microscopy images of the formation of Janus droplets (middle) and the subsequent Janus polymer particles obtained after curing (bottom). From Ref. [7].

Y-junction. Flow rates were tuned so that a two-colored parallel flow was obtained. Then this co-flow stream entered the sheath junction and came into contact with two aqueous streams containing 2 wt.% of PVA. The resulting Janus droplets were collected outside the device and cured by heat-induced polymerization, resulting in Janus polymer particles (Figure 18.13, bottom). In a subsequent study, Nisisako *et al.* [18] pushed further the production of Janus particles by integrating 16 SFMDs

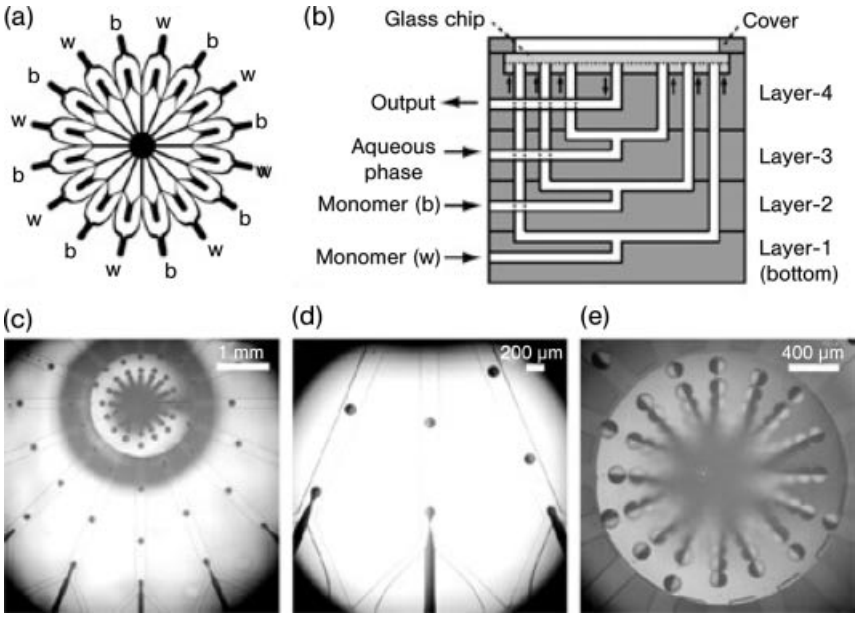

Figure 18.14 Scale-up of production with a 16-channel module. (a) Schematic of the microchannels on a chip. Labels b and w specify the inlet positions for black and white IBA, respectively. The aqueous phase is infused from the inner 16 inlets, arranged circularly. (b) Schematic of internal structure of the holder with a glass chip (side view). (c) Top view of the formation of biphasic droplets in the module. (d) Magnified view of the co-flow geometries. (e) Magnified view of the outlet port in the center of the chip. From Ref. [18].

on a single chip to increase the throughput to 20 g h^{-1} of particles with electrical and color anisotropies (Figure 18.14). The authors claimed that by using many of these systems, several tons per year of such particles could be produced.

Few years later, Weitz and coworkers [19] used the same kind of SFMD for the production of colloid-filled hydrogel granules with controlled size, geometry and composition. Their whole microsystem was made out of PDMS from the replication of a positive relief obtained by the soft lithography technique. The width of the microchannels was set to 100 µm, except for the outlet microchannel, which was 220 µm wide. Two different microchannel heights (150 or 75 µm) allow the synthesis of either spherical or discoidal granules (Figure 18.15). These granules were obtained from the emulsification of an aqueous solution, containing the monomer (acrylamide), a crosslinker (*N*,*N*-methylenebisacrylamide) and a photoinitiator (2,2-diethoxyacetophenone, DEAP), with an oil phase composed of a mixture of hexadecane, mineral oil and in some cases an additional small amount of DEAP. To obtain colloid-filled granules, the authors charged the dispersed phase up to 45 wt.% with silica microspheres (500 nm in diameter)

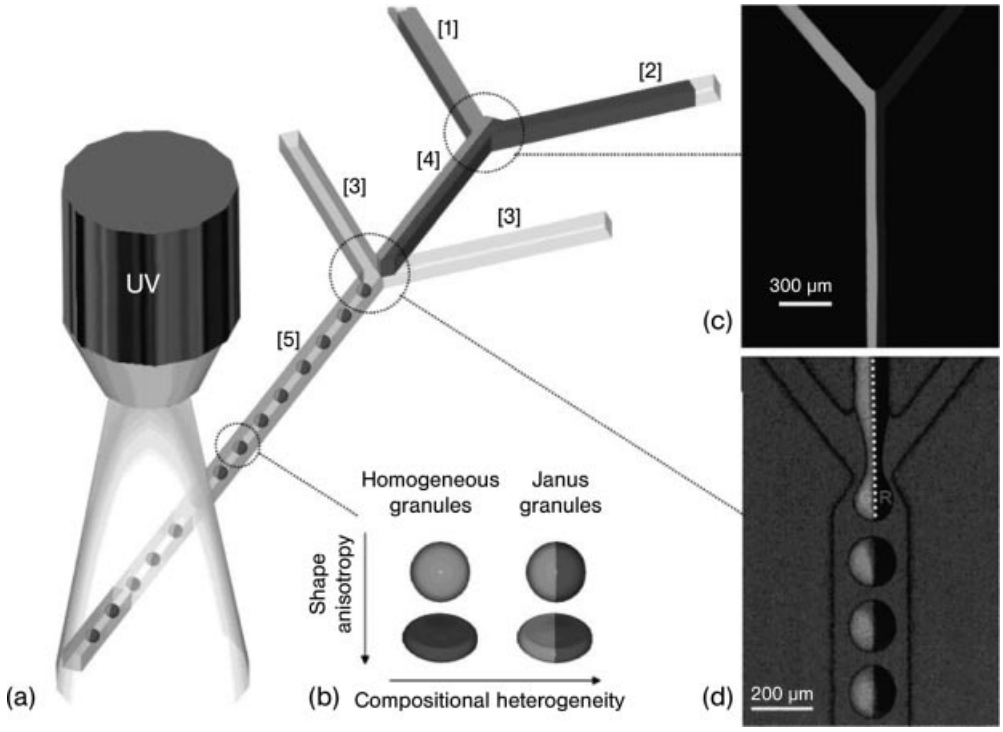

Figure 18.15 (a) Schematic representation of a sheath-flow microfluidic device used to produce monodisperse colloid-filled hydrogel granules; (b) schematic view of granule shapes and compositions explored; (c) fluorescent image of Y-junction formed by inlets [1] and [2] for the production of Janus spheres; and (d) backlit fluorescence image (green excitation) illustrating that the FITC–silica microspheres remain sequestered in the left hemisphere of each granule generated. From Ref. [19].

fluorescently labeled either with rhodamine isothiocyanate (RITC) or fluorescein isothiocyanate (FITC). Depending on the label used in the two streams of aqueous phase entering the Y-junction, the authors were able to obtain homogeneous or Janus droplets at an average frequency of 50 Hz. These droplets were then rapidly UV irradiated in the outlet channel to lead to solid colloid-filled hydrogel granules (Figure 18.16).

A slightly different design of SFMD was used by De Smedt and coworkers [20] for the production of microgels (Figure 18.17, top left). The channels of this microsystem were made of PDMS after replication of a positive relief of the microchannels obtained by soft lithography. Inlet channels were 100 µm wide × 20 µm deep. The width of the flow focusing region was reduced to 10 µm. Microgels were prepared from an aqueous solution containing 30 wt.% of dextran–hydroxyethyl methacrylate (dex-HEMA), 4 vol.% of a nonionic surfactant (cetyl dimethicone copolymer, ABIL

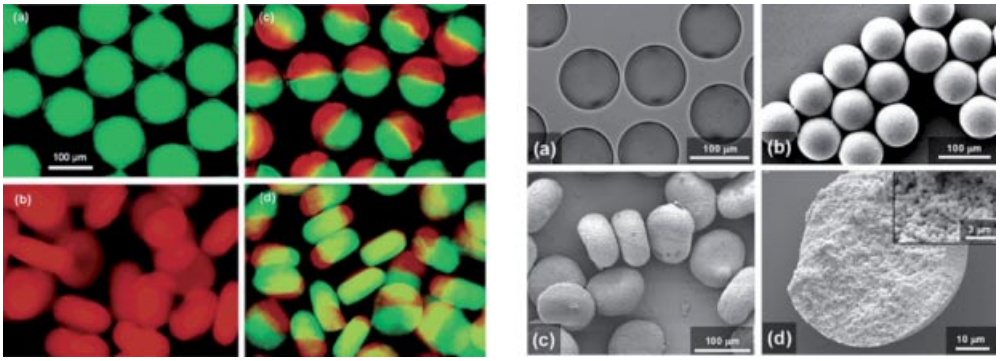

Figure 18.16 Left: fluorescence images of homogeneous (a) spherical and (b) discoidal granules (in oil) and two-excitation fluorescence microscopy images of Janus (c) spherical and (d) discoidal granules (in oil). The images acquired from FITC and RITC excitations are overlaid in (c) and (d). Scale bars are identical for each image. Right: (a) Optical micrograph of pure hydrogel spheres (in oil); (b, c) scanning electron micrographs of dried spherical and discoid granules; and (d) scanning electron micrograph of a dried, freeze-fractured spherical granule. Inset in (d) depicts a higher magnification view of the random close-packed network of silica microspheres within the dried granule. From Ref. [19].

EM-90) and a photoinitiator (Irgacure 2959, Ciba). The continuous phase was a mineral oil. Surfactant was used to reduce the surface tension between both phases and helped in obtaining a regular and clean droplet break-off (Figure 18.17, bottom), otherwise co-flowing laminar streams are observed (Figure 18.17, top right). Once emulsified, the droplets of dex-HEMA were collected and immediately UV irradiated while still suspended within oil. This microsystem-assisted process allows for the production of monodisperse microgel particles (Figure 18.18, left) having a mean diameter of 10 µm (Figure 18.18, middle) at a relative frequency of 10–100 Hz. In contrast, the emulsification of the same aqueous solution in a conventional batch reactor produces particles with a large size distribution (Figure 18.18, right). Particles of dex-HEMA are biodegradable and can degrade by hydrolysis of the carbonate ester groups. Therefore, they are suitable for protein encapsulation and controlled drug delivery.

18.3.4
Projection Photolithography Devices

The projection photolithography technique was developed at first by Doyle and coworkers [21] for the production of non-spherical, shape-controlled polymer particles (Figure 18.19) with a spatial resolution of typically 3 µm. Their first set of experiments consisted in UV irradiation through different mask patterns of an acrylate oligomer solution [poly(ethylene glycol diacrylate), PEG-DA] containing 5 vol.% of a photoinitiator (Darocur 1173) flowing in an all-PDMS rectangular

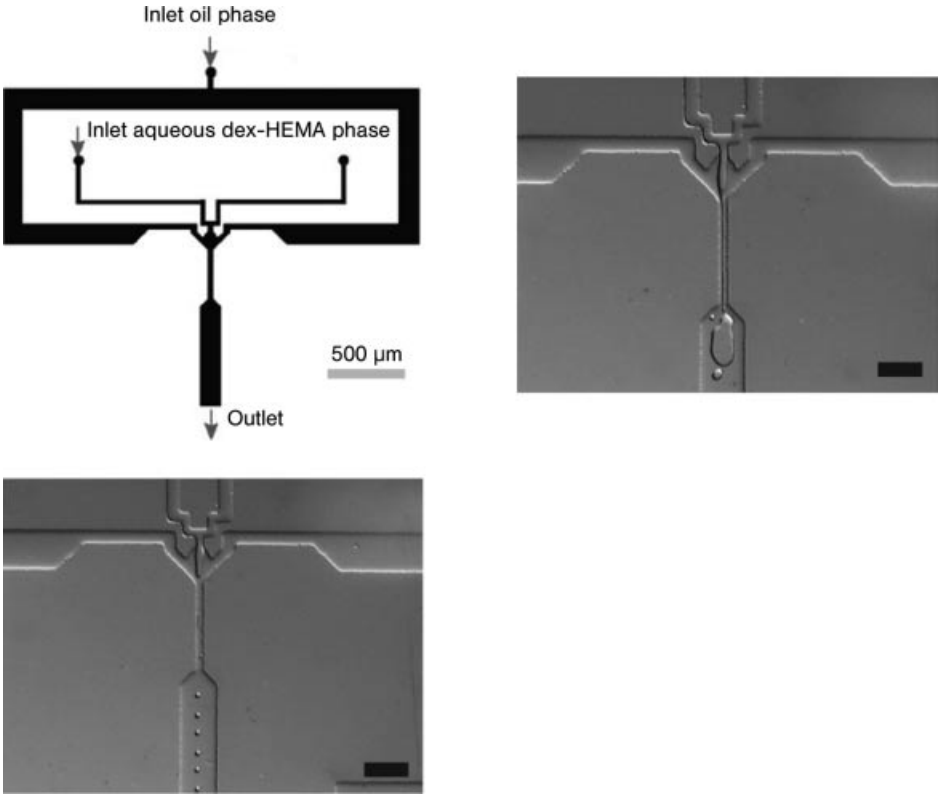

Figure 18.17 Top left: schematic representation of the microsystem used for the production of biodegradable microgels. Top right: insufficient shear between the aqueous dex-HEMA and mineral oil phases resulted in co-flowing laminar streams. Bottom: the addition of surfactant in the continuous oil phase facilitated regular droplet break-off. From Ref. [20].

microchannel. The latter was obtained by pouring PDMS on a silicon wafer containing the positive relief of the microchannel patterned in SU-8 photoresist and sealed with a glass slide on which PDMS had been spin-coated. Microchannels with different dimensions were fabricated (200, 600 and 1000 µm widths and 9, 6, 20 and 38 µm depths).

In another study, Doyle and coworkers [22] used a Y-junction to establish the concurrent flow of a hydrophilic monomer stream with a hydrophobic monomer stream (Figure 18.20, top). The hydrophobic solution was composed of trimethylolpropane triacrylate (TMPTA) and the hydrophilic phase was composed of 65 vol.% of PEG-DA in water. Both solutions were formulated with 5 vol.% of a photoinitiator (Darocur 1173). Then they synthesized amphiphilic biphasic particles simply by UV irradiating across the interface. The mask they used allows shaping of particles with a hydrophilic head and a hydrophobic tail (Figure 18.20, middle). Due to their unique

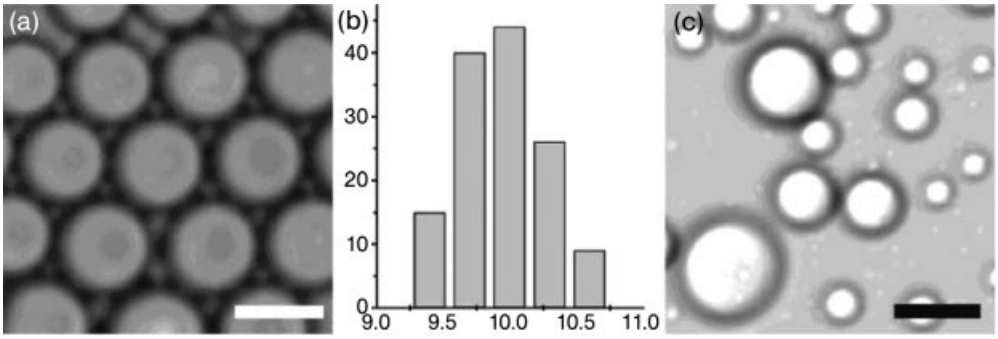

Figure 18.18 (a) Optical microscopy images of monodisperse dex-HEMA microgels synthesized using the microsystem. (b) Size distribution of the monodisperse microgels. (c) Polydisperse microgels obtained by ordinary emulsification of the equivalent solution in mineral oil. From Ref. [20].

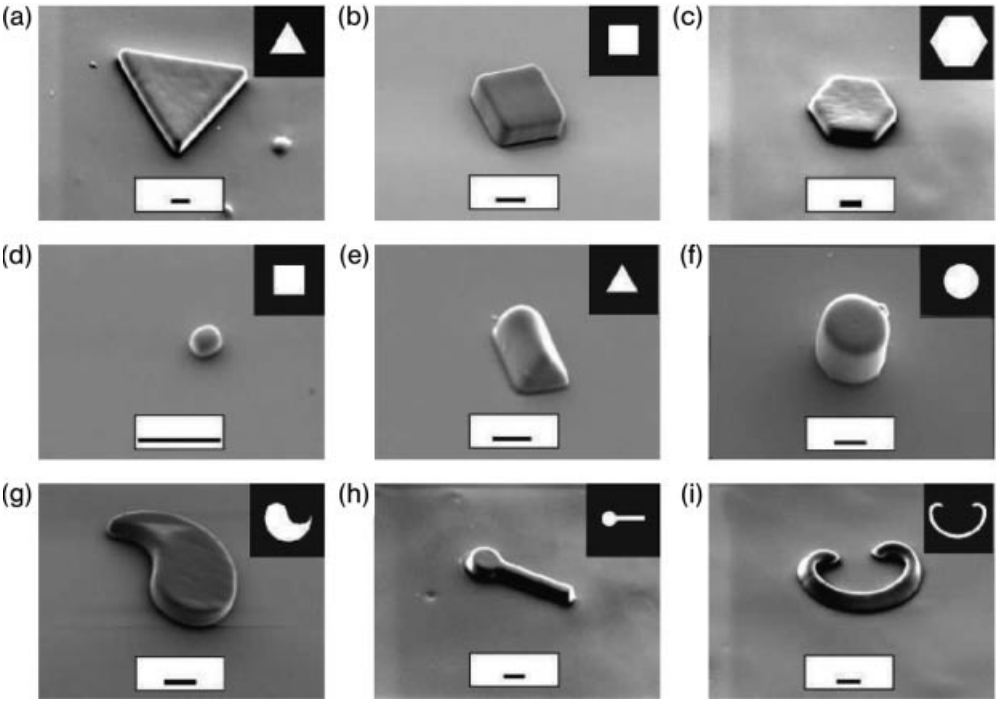

Figure 18.19 SEM images of the different particles synthesized; the inset represents the mask pattern used for that particle; the scale bar is 10 μm. From Ref. [21].

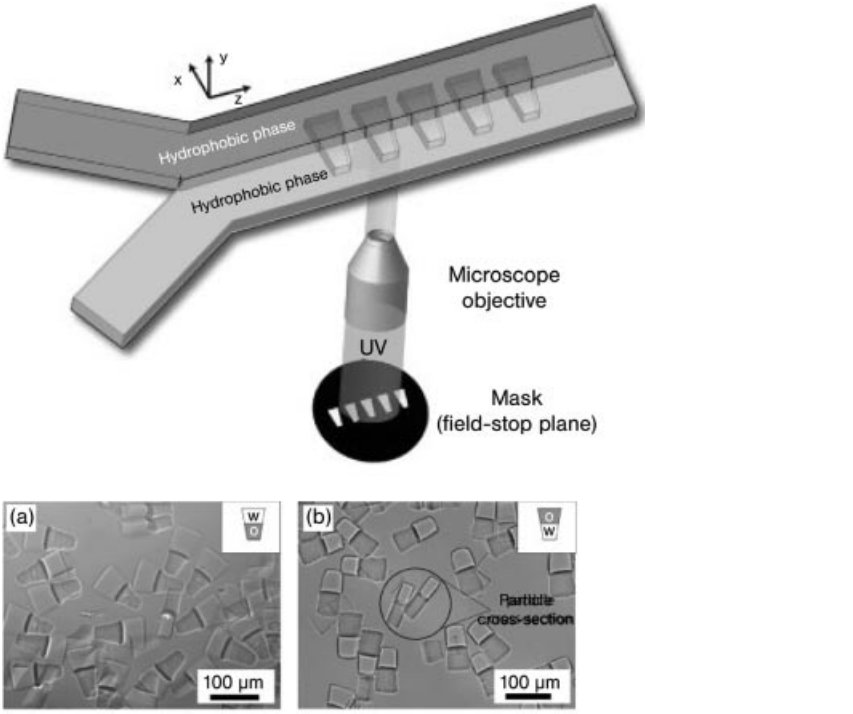

Figure 18.20 Top: schematic depicting the Y-junction for the laminar co-flow of hydrophobic and hydrophilic streams. Middle: optical images of amphiphilic particles as seen by differential interference contrast (a, b, e); particles with a large hydrophilic head and a small hydrophobic tail (a); particles with a small hydrophilic head and a large hydrophobic tail (b); SEM images of particles as seen in a (c) or in b (d); ball-and-stick model biphasic particles with a hydrophilic disk-shaped head and a long hydrophobic tail (e). Bottom: particles with a large hydrophilic head and a small hydrophobic tail cluster in a bath of TMPTA (a); particles as seen in a form a micelle-like structure in water (b); particles with a large hydrophilic head and a small hydrophobic tail assemble at the interface of an oil-in-water and a water-in-oil emulsion [(c) and (d), respectively]. From Ref. [22].

amphiphilic property and shape, particles self-assemble to minimize their surface energy. The structure formed depends on the properties of the surrounding fluid (Figure 18.20, bottom). With this technique, the proportion of each monomer in the final particle can be varied either by changing the relative flow rate of the two monomer solutions (to displace the interface) or by moving the irradiated spot.

18.4 Conclusion

From the above-reported recent studies, there is no doubt that microfabricated systems represent new, promising tools for the production of size- and shape-

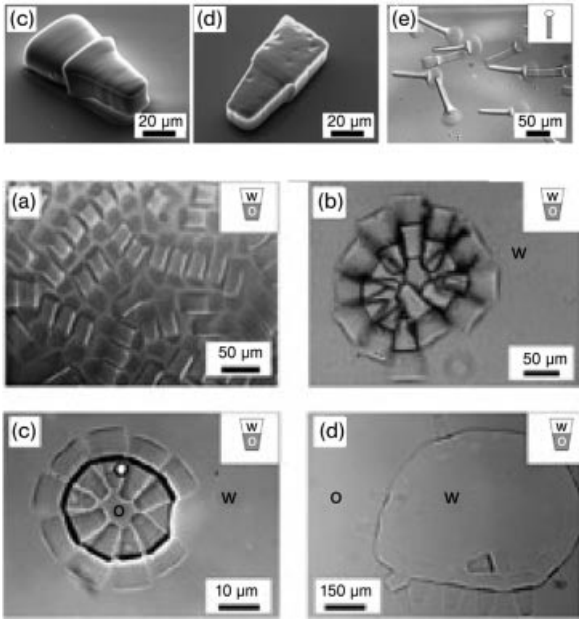

Figure 18.20 (*Continued*).

controlled polymer particles. Furthermore, particles with new morphologies and multicomponent compositions – such as Janus, ternary, multicored and colloid-filled particles – can only be prepared in such systems. It is believed that these microsystems will enable or push forward new applications in fields such as drug delivery, electronic displays and photonics. Moreover, they will probably help to improve the knowledge on the mechanisms which induce the micro/nanostructures of complex polymer particles.

References

1 S. Sugiura, M. Nakajima, H. Itou, M. Seki, *Macromol. Rapid Commun.* **2001**, *22*, 773–778.

2 S. Sugiura, M. Nakajima, M. Seki, *Ind. Eng. Chem. Res.* **2002**, *41*, 4043–4047.

3 T. Kawakatsu, Y. Kikuchi, M. Nakajima, *J. Am. Oil. Chem. Soc.* **1997**, *74* (3), 317–321.

4 F. Ikkai, S. Iamoto, E. Adachi, M. Nakajima, *Colloid Polym. Sci.* **2005**, *28*, 1149–1153.

5 T. Thorsen, R. Roberts, F. Arnold, S. Quake, *Phys. Rev. Lett.* **2001**, *86*, 4163–4166.

6 T. Nisisako, T. Torii, T. Higuchi, *Lab Chip* **2002**, *2*, 24–26.

7 T. Nisisako, T. Torii, T. Higuchi, *Chem. Eng. J.* **2004**, *101*, 23–29.

8 D. Dendukuri, K. Tsoi, A. Hatton, P. S. Doyle, *Langmuir* **2005**, *21*, 2113–2116.

9 M. Zourob, S. Mohr, A. G. Mayes, A. Macaskill, N. Pérez-Moral, P. R. Fielden, N. J. Goddard, *Lab Chip* **2006**, *6*, 296–301.

10 A. Kubo, H. Shinmori, T. Takeuchi, *Chem. Lett.* **2006**, *35*, 588–589.

11 S.L. Anna, N. Bontoux, H.A. Stone, *Appl. Phys. Lett.* **2003**, *82*, 264–366.

12 M. Seo, Z. Nie, S. Xu, M. Mok, P.C. Lewis, R. Graham, E. Kumacheva, *Langmuir* **2005**, *11*, 11614–11622.

13 M. Seo, Z. Nie, S. Xu, P. C. Lewis, E. Kumacheva, *Langmuir* **2005**, *21*, 4773–4775.

14 S. Q. Xu, Z. H. Nie, M. Seo, P. Lewis, E. Kumacheva, H. A. Stone, P. Garstecki, D. B. Weibel, I. Gitlin, G. M. Whitesides, *Angew. Chem. Int. Ed.* **2005**, *44*, 724–728.

15 P. C. Lewis, R. R. Graham, Z. Nie, S. Xu, M. Seo, E. Kumacheva, *Macrolecules* **2005**, *38*, 4536–4538.

16 Z. Nie, S. Xu, M. Seo, P. C. Lewis, E. Kumacheva, *J. Am. Chem. Soc.* **2005**, *127*, 8058–8063.

17 Z. Nie, W. Li, M. Seo, S. Xu, E. Kumacheva, *J. Am. Chem. Soc.* **2006**, *128*, 9408–9412.

18 T. Nisisako, T. Torii, T. Takahashi, Y. Takizawa, *Adv. Mater.* **2006**, *18*, 1152–1156.

19 R. F. Shepherd, J. C. Conrad, S. K. Rhodes, D. R. Link, M. Marquez, D. A. Weitz, J. A. Lewis, *Langmuir* **2006**, *22*, 8618–8622.

20 B. G. De Geest, J. P. Urbanski, T. Thorsen, J. Demeester, S. De Smedt, *Langmuir* **2005**, *21*, 10275–10279.

21 D. Dendukuri, D. C. Pregibon, J. Collins, T. A. Hatton, P. S. Doyle, *Nat. Mater.* **2006**, *5*, 365–369.

22 D. Dendukuri, T. A. Hatton, P. S. Doyle, *Langmuir* **2007**, *23*, 4669–4674.